Modeling of a semiconductor laser coupled to an external fiberoptic ring resonator

Dmitry A. Korobko, Igor O. Zolotovsky, Krassimir Panajotov, Vasily V. Spirin, Andrei A. Fotiadi

Dmitry A. Korobko, Igor O. Zolotovsky, Krassimir Panajotov, Vasily V. Spirin, Andrei A. Fotiadi, "Modeling of a semiconductor laser coupled to an external fiberoptic ring resonator," Proc. SPIE 10682, Semiconductor Lasers and Laser Dynamics VIII, 106821V (9 May 2018); doi: 10.1117/12.2307217

SPIE.

Event: SPIE Photonics Europe, 2018, Strasbourg, France

Modeling of a semiconductor laser coupled to an external fiber-optic ring resonator

Dmitry A. Korobko*[a], Igor O. Zolotovsky [a], Krassimir Panajotov [b], Vasily V. Spirin [c] and Andrei A. Fotiadi [a, d, e]

a Ulyanovsk State University, 42 Leo Tolstoy Street, Ulyanovsk, 432970, Russian Federation
b Brussels Photonics Team, Department of Applied Physics and Photonics (B-PHOT TONA), Vrije Universiteit Brussels, Pleinlaan 2, 1050 Brussels, Belgium
c Scientific Research and Advanced Studies Center of Ensenada (CICESE), Carretera Ensenada-Tijuana No. 3918, Zona Playitas, 22860 Ensenada, B.C., México
d University of Mons, blvd. Dolez 31, Mons, B-7000, Belgium
e Ioffe Physical-Technical Institute, 26 Politekhnicheskaya, St Petersburg 194021, Russian Federation

ABSTRACT

Self-injection locking, an efficient method to improve the spectral performance of semiconductor lasers without active stabilization, has already demonstrated its high potential for operation with single-longitude-mode fiber lasers urgently demanded by new applications in optical metrology and spectroscopy, coherent optical communications, distributed fiber sensing. The laser operation stability remains to be a crucial issue for such laser applications. Here, we present a theoretical framework for modeling of semiconductor laser coupled to an external fiber-optic ring resonator. The developed approach has shown good qualitative agreement with theoretical predictions and experimental results for particular configuration of a self-injection locked DFB laser delivering narrow-band radiation and particular employed in Brilloin fiber laser configurations. The model is capable of describing the main features of the experimentally measured laser outputs such as laser line narrowing, spectral shape of generated radiation, mode-hoping instabilities and makes possible exploring the key physical mechanisms responsible for the laser operation stability.
Keywords: Injection-locked oscillators, semiconductor lasers, fiber lasers, resonator filters

1. INTRODUCTION

Linewidth narrowing and stabilization of semiconductor laser light generation are of topical research concern governed by the great needs of compact unexpensive narrow-band laser sources for a number of potential applications. Among them are phase coherent optical communications, distributed fiber optics sensing, high-resolution spectroscopy, coherent optical spectrum analyzing, and microwave photonics [1-5]. Self-injection locking of a semiconductor laser through an external feedback is one of the most promising mechanisms for the laser line narrowing [6, 7]. To provide the effect, a part of the optical radiation emitted by the laser should be returned back into the laser cavity. This relatively simple technique allows to design cost-effective narrow-band laser sources based on standard laser diodes making them an attractive solution in comparison with traditional laser systems based on an active feedback.

Usually, self-injection locking laser configuration comprises a narrow bandpass optical filter inside a weak feedback loop. Recent progress in this topic is associated with the use of micro-cavity techniques [8]. Employing optical

Semiconductor Lasers and Laser Dynamics VIII, edited by Krassimir Panajotov, Marc Sciamanna, Rainer Michalzik,
Proc. of SPIE Vol. 10682, 106821V · © 2018 SPIE · CCC code: 0277-786X/18/$18 · doi: 10.1117/12.2307217

whispering-gallery-mode resonators the linewidth of the semiconductor laser could be decreased down to Hz range in a compact and robust format [9]. However, the external cavities employed in such systems possessing extremely high Q-factors (~10^{11}) are not adjustable and require complicate coupling of fiber and non-fiber elements. Instead, all-fiber cavity solutions based on long, but relatively low-Q-factor resonators, in particular fiber ring resonators [10, 11] are able to provide comparable semiconductor laser line narrowing employing rather cheap fiber configuration built from standard telecom components. In particular, such solutions are of great interest for Brillouin fiber lasers because the same fiber cavity can serve as nonlinear medium to generate Brillouin frequency-shifted light [12-19]. Another important area are random fiber lasers, where narrow-band semiconductor lasers are commonly used as a pump source [20-28]. In such systems even a week backward effect of the laser cavity on the pumping diode could significantly contribute the random laser dynamics. Recently, we have demonstrated 1000-fold line-narrowing of a conventional low-cost DFB laser locked to an external fiber optic ring resonator [29]. However, events of rare mode-hopping have been found to interrupt the stable laser operation making its practical application questionable [29, 30]. Therefore, the advanced understanding of the physical mechanisms responsible for the operation of the laser-feedback cavity system is of great practical importance for further laser configuration designs.

Semiconductor lasers with an external feedback are complex dynamical systems demonstrating a wide range of generation regimes varying from a stable light generation, to periodic and quasi-periodic oscillations and to chaotic lasing [31, 32]. The laser dynamics have already been considered in some system configurations, including the case of a feedback through a narrow-band frequency filter [33, 34]. However, an appropriate approach for describing semiconductor laser coupled to an external optical fiber ring resonator has not been developed yet. A specific feature of this system is the very narrow linewidth of the generated light that is at least 3 orders of magnitude narrower than the linewidth of the solitary semiconductor laser. Besides, for a typical several-meter long fiber ring cavity several peaks of the fiber resonators transmittance spectrum compete for the laser generation making mode hopping probable. In the present work we report a theoretical description of a semiconductor laser optically coupled to a ring fiber resonator taking into account multi-peak spectral performance of the external filtering. Our simulation results explore key features of the laser dynamics important for advanced understanding of the physical mechanisms responsible for laser instabilities and suitable for qualitative explanation of experimental observations.

2.THEORETICAL MODEL

The experimental configuration of a semiconductor laser coupled to a fiber-optic ring resonator is shown in Fig.1. The laser diode operates the wavelength near 1.55 μm. The diode is supplied by a built-in optical isolator attenuating the power of backward radiation by ~30 dB. Without such an isolation the semiconductor laser is extremely sensitive to parasitic backreflections from fiber splices and connectors and backward Rayleigh scattering that disturb stable laser operation and could lead to periodic, quasi-periodic or chaotic light generation [31, 32]. The built-in optical isolator eliminates the effects of uncontrollable backreflections and simultaneously reduces the value of a controllable feedback from the external fiber optic ring resonator. To implement the injection locking mechanism, the light emitted by the laser passes an optical circulator (OC) and is introduced through a coupler C1 into a ring cavity. The ring fiber cavity is spliced from couplers C1 (90/10) and C2 (99/1) and comprises totally 4 m length of standard SMF-28 fiber. The coupler C2 is used to redirect a part of the light circulating in the cavity through circulator (OC) back into the DFB laser providing a feedback for self-injection locked laser operation. The typical width of the locked laser spectrum measured by the delayed self-heterodyne method is ~ 2.4 kHz [29]. Commonly, a stable self-injection locking regime is observed during 1 – 100 s (depending on environment noise level). It is periodically interrupted by mode-hopping events making the laser unstable during typically ~5 ms [29, 30].

To describe the laser operation we consider a system consisting of a semiconductor laser and a fiber ring resonator connected though the feedback loop. Further analysis is valid for both Fabry-Perot (FB) and distributed feedback (DFB) semiconductor lasers, as long as the power coupling coefficient in DFB cavity periodic structure could be described by an output mirror reflectivity of an equivalent Fabry-Perot laser cavity. For example, a coupling coefficient of the DFB

laser of $\sigma L = 2.2$ corresponds to a reflection coefficient of the external mirror of the FP laser of $R = 0.32$ [32]. The whole light frequency range under consideration is limited by ~100 MHz that covers several modes of the ring resonator of several meters long. The typical light round trip time in a semiconductor FP cavity is a few ps. For the DFB laser with the same length of the cavity this value is lower, but of the same order of magnitude. The solitary semiconductor laser operation is assumed to be single-frequency, which is a natural property of the DFB laser diode. The free spectral range (FSR) of the semiconductor laser is in GHz range, so only one, the most successful longitudinal mode possessing the highest gain and the lowest generation threshold is under consideration. Effects associated with light polarization are not taken into account, i.e. laser light is considered to be linearly polarized and all fiber components (fiber lengths, couplers, a circulator) are assumed to be polarization maintaining [30].

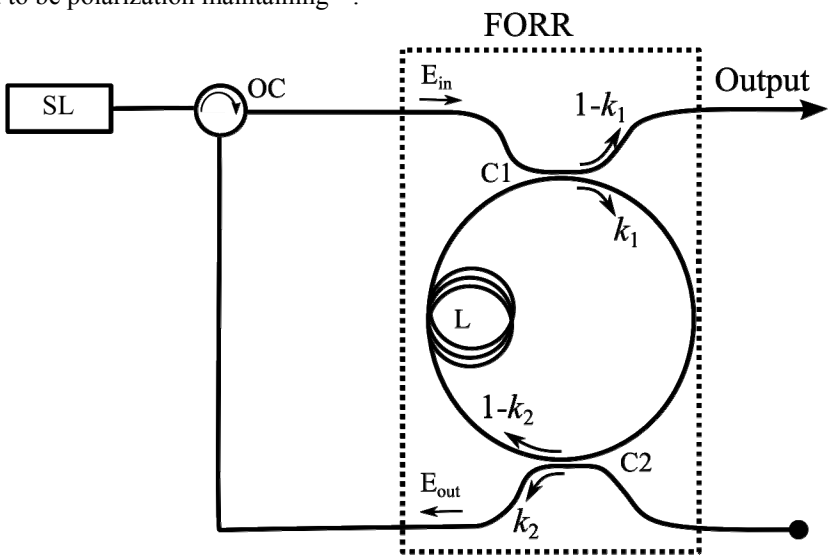

Figure 1. Experimental configuration of the semiconductor laser coupled to a fiber-optic ring resonator (FORR); OC- optical circulator, C1, C2 – optical couplers.

According to [35] the number of photons S, the phase of optical field φ, and the number of carriers n in the semiconductor laser cavity could be described by Lang-Kobayashi type laser rate equations:

$$\begin{aligned}
\frac{dS}{dt} &= \left(G(n-n_0) - \frac{1}{\tau_p} \right) S + Q + 2k_c \sqrt{f_{ext}} \sqrt{S(t)S(t-\tau_0)} \cdot \cos\left(\omega_0 \tau_0 + \varphi(t) - \varphi(t-\tau_0)\right) + F_s(t) \\
\frac{d\varphi}{dt} &= \frac{1}{2} \alpha G(n-n_{th}) - k_c \sqrt{f_{ext}} \sqrt{\frac{S(t-\tau_0)}{S(t)}} \cdot \sin\left(\omega_0 \tau_0 + \varphi(t) - \varphi(t-\tau_0)\right) + F_\varphi(t) \\
\frac{dn}{dt} &= \frac{I - I_{th}}{e} - \frac{n}{\tau_s} - G(n-n_0)S + F_n(t)
\end{aligned} \tag{1}$$

Here, e is the elementary charge, τ_s is the carrier lifetime, τ_p is the photon lifetime, τ_0 is the roundtrip delay time of the external cavity, k_c is the parameter determined by the reflection coefficient of the semiconductor laser cavity R and the cavity roundtrip time $\tau_L = 2n_p L_D / c$:

$$k_c = \frac{1}{\tau_L} \frac{1-R}{\sqrt{R}} \tag{2}$$

f_{ext} is the power fraction of light returned to the cavity, ω_0 is the central frequency of a solitary semiconductor laser

at the generation threshold, α is the semiconductor linewidth enhancement factor, $I - I_{th}$ is the difference between the laser pump current and its threshold value. The gain is presented in a linear approximation for the number of non-equilibrium carriers n, i.e. $g = G(n - n_0)$, where n_0 is the number of non-equilibrium carriers corresponding to zero amplification, G is the differential gain, and n_{th} is the number of non-equilibrium carriers at the generation threshold. The term $Q = \beta/\tau_p$ describes spontaneous emission, where β is the inversion coefficient, F_i are the terms describing the Langevin noise source of a Gaussian statistics simulated through a random number generator [36]. The parameters used for the numerical simulations describe a typical semiconductor lasers and are listed in Table 1.

Table 1. Parameters for calculations (semiconductor laser)

Symbol	Quantity	Value
L_D	semiconductor cavity length	300 μm
n_p	semiconductor cavity refractive index	3.53
α	semiconductor linewidth enhancement factor	5
τ_s	carrier lifetime	2 ns
τ_p	photon life time	4 ps
R	reflection of the rear semiconductor laser cavity mirror	0.32
n_0	number of non-equilibrium carriers corresponding to zero amplification	10^8
G	differential amplification,	10^4 s^{-1}
β	inversion coefficient	2.2
$\lambda_0 = 2\pi \frac{c}{\omega_0}$	central wavelength of a solitary laser generation at the threshold	1550 nm
I_{th}	threshold current	15 mA
I	pump current	17 mA

The values of S_{th} and n_{th} corresponding to the generation threshold of a solitary semiconductor laser could be analytically found from (1) through its steady-state solution. Numerical simulations of (1) have been performed employing 4-order Runge-Kutta algoritm and resulted in time series of the number of photons $S(t)$, carriers $n(t)$, and the phase of optical field $\varphi(t)$. These data have been used for reconstruction of the laser spectrum determined as a Fourier transforms of the complex field amplitude.

For the laser operating with a feedback the threshold gain and the generation frequency are determined from (1) by the power fraction returned to the resonator f_{ext} and by the feedback phase

$$\begin{aligned} \Delta g &= -2k_c\sqrt{f_{ext}}\cos(\omega\tau_0), \\ (\omega - \omega_0)\tau_0 &= -C\sin(\omega\tau_0 + \arctan\alpha), \end{aligned} \tag{3}$$

where $\omega = d\varphi/dt$ and $C = k_c\tau_0\sqrt{f_{ext}(1+\alpha^2)}$. The laser generation linewidth is linked to the linewidth of a solitary

laser as $\delta\upsilon \sim \delta\upsilon_0 \Big/ \left(1 + C\cos\left(\omega\tau_0 + \arctan\alpha\right)\right)^2$ [31, 32, 35].

These expressions highlight the effects of the feedback loop on the laser stabilization and laser line narrowing. Depending on the parameter C several laser operation regimes are possible. For $C < 1$ the laser linewidth is determined mainly by the feedback phase $\omega\tau_0$ (mode I). With an increase of the feedback power fraction f_{ext}, in an intermediate case $C \geq 1$, a narrowing of the laser line (mode II) occurs. With further f_{ext} increase $C >> 1$ the laser frequency is locked to $\omega\tau_0 = 2\pi - \arctan\alpha$ providing the narrowest laser generation line (mode III). The last regime is limited by a certain value of f_{ext} above which the so-called "collapse of coherence" accompanied by a significant broadening of the generation line occurs (regime IV) [31].

Table 2. Parameters for calculations (fiber ring cavity)

Symbol	Quantity	Value
L_r	optical fiber ring cavity length	4 m
L_s	length of the external connection fiber	2.56 m
n_f	fiber refractive index	1.5
l_{ext}	feedback loop transmittance	$0 \ldots 4 \cdot 10^{-4}$
k_1	power coupling coefficient (C1)	0.1
k_2	power coupling coefficient (C2)	0.01
γ_1, γ_2	losses in couplers	0.1 dB
δ	power transmission coefficient of the ring cavity fiber	0.35 dB

Let us consider a semiconductor laser with a feedback loop comprising a narrow-band pass filter. In contrast to previous considerations employing filters with a single Lorentz profile [33], here, a frequency filter comprising several transmission lines of the fiber ring resonator should be taken into account. The amplitude reflection coefficient of the ring resonator $k_{ext}(\omega)$ relates the amplitudes of the fields entering and exiting the ring resonator $E_{out} = k_{ext} E_{in}$ (Fig. 1) and thus determines the spectral performance of the power fraction returned to the semiconductor laser cavity $f_{ext} = \left|k_{ext}\right|^2 \cdot l_{ext}$, where l_{ext} is the spectrally uniform feedback loop transmission coefficient mainly determined by the losses in the laser build-in optical isolator (~30 dB). The spectrally selective reflection coefficient can be expressed as [29]

$$k_{ext}(\omega) = \frac{\sqrt{(1-\gamma_1)k_1 k_2}\exp(\mathrm{i}\omega\tau_r)}{\sqrt{\delta(1-\gamma_1)(1-k_1)} - \exp(\mathrm{i}\omega\tau_r)} \tag{4}$$

Here k_1, k_2 are power coupling coefficients of couplers C1 and C2, respectively, $\delta = (1-k_2)10^{-(\varsigma+\gamma_2)/10}$ is the power transmission coefficient of the ring resonator (dB) determined by losses in the coupler (C2) and losses ς in the fiber splices inside the ring resonator (losses inside the fiber are negligibly small), γ_1, γ_2 are the loss factors in the couplers. The parameters used for the ring resonator correspond to its operation in the critical coupling regime [29] and are listed in Table 2.

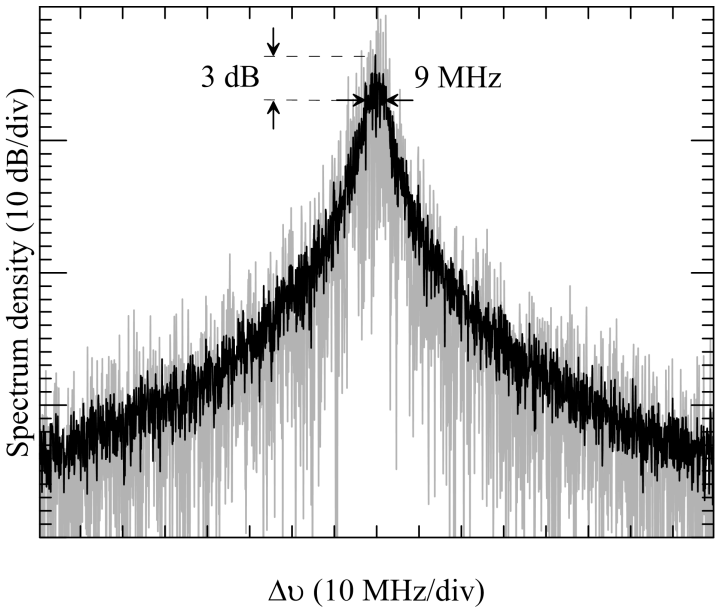

Figure 2. Spectrum of the semiconductor laser without feedback: a typical spectrum realization (grey) and the spectrum averaged over 10 noise realizations (black).

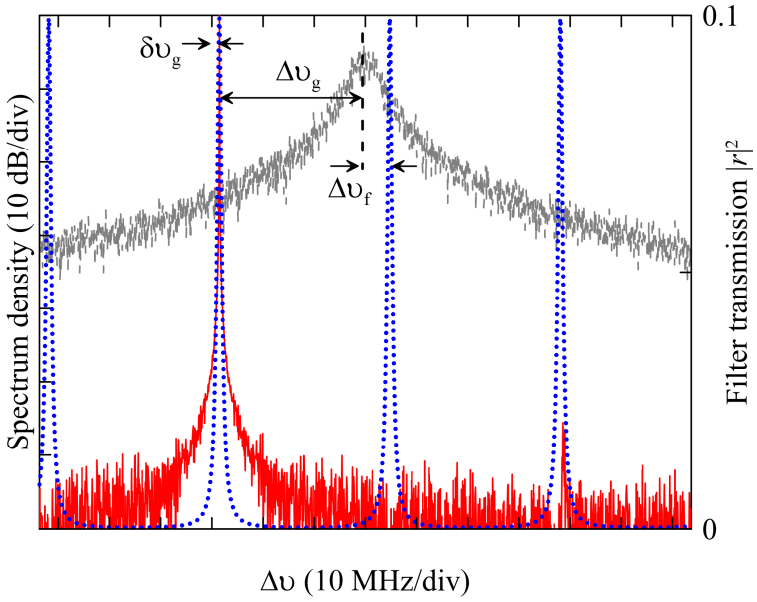

Figure 3. Spectrum of the semiconductor laser with optical feedback from fiber ring resonator (red), a solitary laser spectrum (grey) and the transmission spectrum $|k_{ext}|^2$ of the ring interferometer (blue) calculated for the ring resonator with a length of $L_r = 4$ and the feedback loop transmission of $l_{ext} = 4 \cdot 10^{-4}$.

To take the multi-peak performance of the resonant filtering into account the corresponding terms in (1) must be presented as convolutions describing the response of S and φ on passing light through the ring resonator. Thus, the

feedback terms on the right-hand side of (1) are presented as

$$k_c\sqrt{l_{ext}}\int_0^{t-\tau_0-\tau_r} d\tau\,|k_{ext}(\tau)|\sqrt{S(t)S(t-\tau_0-\tau_r-\tau)}\cdot\cos\left(\omega_0(\tau_0+\tau_r+\tau)+\varphi(t)-\varphi(t-\tau_0-\tau_r-\tau)+\arg(k_{ext}(\tau))\right)$$

$$k_c\sqrt{l_{ext}}\int_0^{t-\tau_0-\tau_r} d\tau\,|k_{ext}(\tau)|\sqrt{S(t-\tau_0-\tau_r-\tau)/S(t)}\cdot\sin\left(\omega_0(\tau_0+\tau_r+\tau)+\varphi(t)-\varphi(t-\tau_0-\tau_r-\tau)+\arg(k_{ext}(\tau))\right)$$

Here $\tau_0 = n_f L_s/c$ is the delay time in the connecting feedback loop fiber, $\tau_r = n_f L_r/c$ is the delay time in the ring resonator, n_f is the fiber refractive index, $k_{ext}(\tau)$ is the feedback source function obtained as the inverse Fourier transform applied to $k_{ext}(\omega)$. Note that this function is nonzero only for moments of time corresponding to full round-trips of the ring resonator $\tau = m\cdot\tau_r$, $m = 0, 1, \ldots +\infty$.

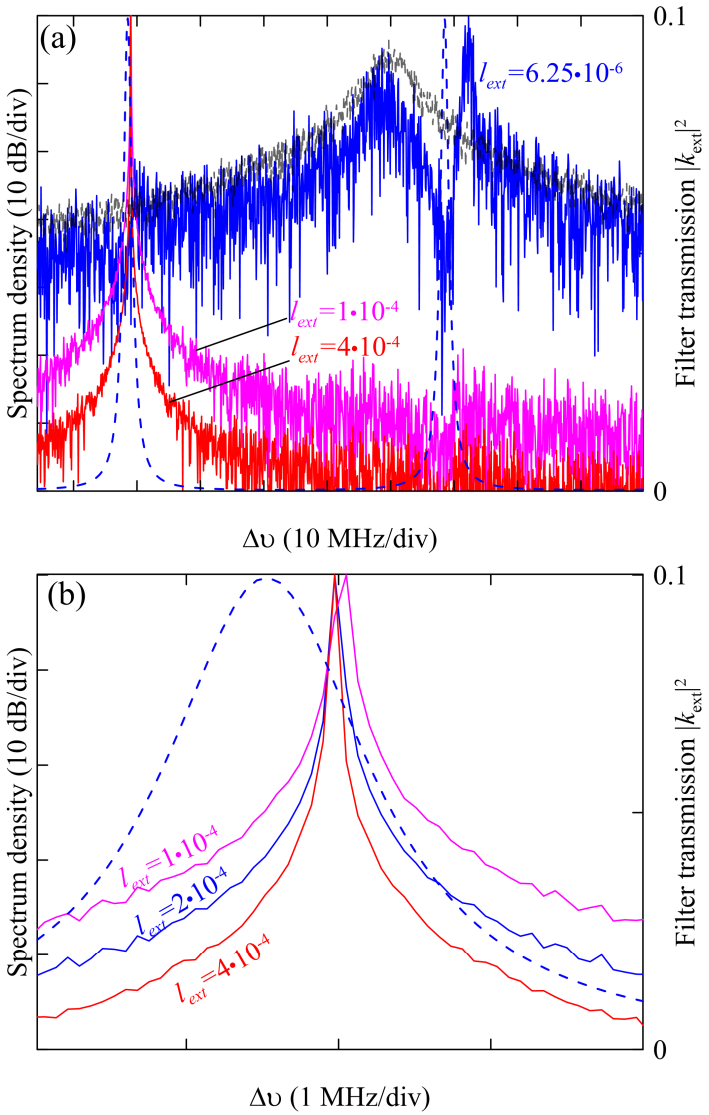

Figure 4. (a) Evolution of the laser spectrum at different feedback levels. The spectrum of a solitary laser (grey) and the transmission spectrum (blue) of the ring interferometer are also shown. (b) Zoom of (a) near the transmission peak.

3. NUMERICAL ANALYSIS

Figure 2 shows a typical spectrum generated by the solitary semiconductor laser without feedback. It is calculated by the traditional form of Eq. (1). The spectrum averaged over ten independent noise realizations is shown for comparison. The FWHM of the solitary laser line is about 9 MHz.

After rewriting the feedback terms as integrals, the numerical results demonstrating the laser configuration with FORR are illustrated in Fig. 3. In these simulations, we set a difference of $\Delta\upsilon_f = 8.5 MHz$ between the nearest spectral peak of the ring resonator and the threshold solitary laser frequency $\omega_0/2\pi$. One can see however, that the laser generates around another peak of the ring resonator. The feedback causes a decrease of the laser threshold power and forces the laser to generate at the nearest ring resonator mode at lower frequency. The difference between the laser generation frequency and the solitary laser threshold frequency is $\Delta\upsilon_g = -41\, MHz$ and the FWHM of the generation line is less than 20 kHz. Thus, the laser line is narrowed by more than 450 times. It should be noted however, that the spectrum resolution in this case is limited by $d\upsilon \approx 20 kHz$ determined by the duration of the calculated time series comprising 2^{20} time points with a step of 50 ps. An improvement of the spectral resolution is numerically too time-demanding.

From Fig. 3 one can also see that the decrease of the generation threshold occurs for only one resonator mode. This is caused by a constructive interference of the generated cavity field and the feedback radiation achieved inside the semiconductor laser cavity. On the contrary, at frequencies corresponding to other neighboring modes a destructive interference increases the generation threshold. For the rest of the laser spectrum, the threshold is not affected that finally results in a decrease of the relative noise level. In particular, for the case shown in Fig. 3 the noise level is reduced by more than 30 dB.

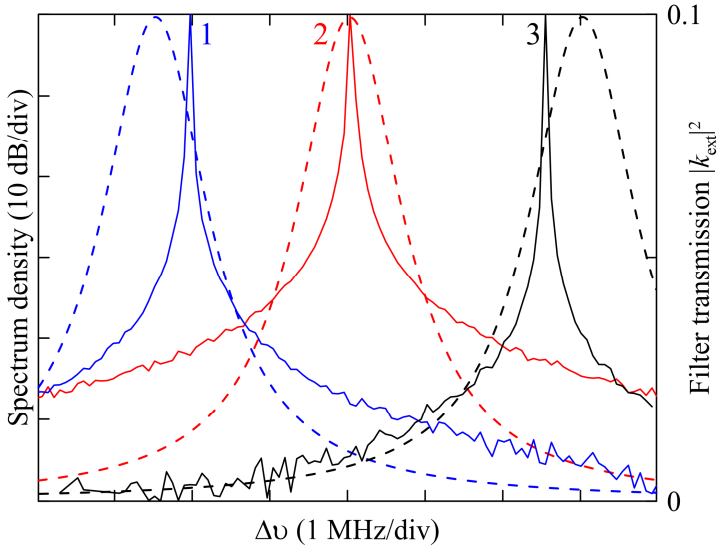

Figure 5. The laser spectrum (solid curves) and the ring interferometer transmission spectrum (dotted curves) at different detuning $\Delta\upsilon_f$: 1 – $\Delta\upsilon_f = 8.5\, MHz$, 2 – $\Delta\upsilon_f = 11\, MHz$, 3 – $\Delta\upsilon_f = 14\, MHz$

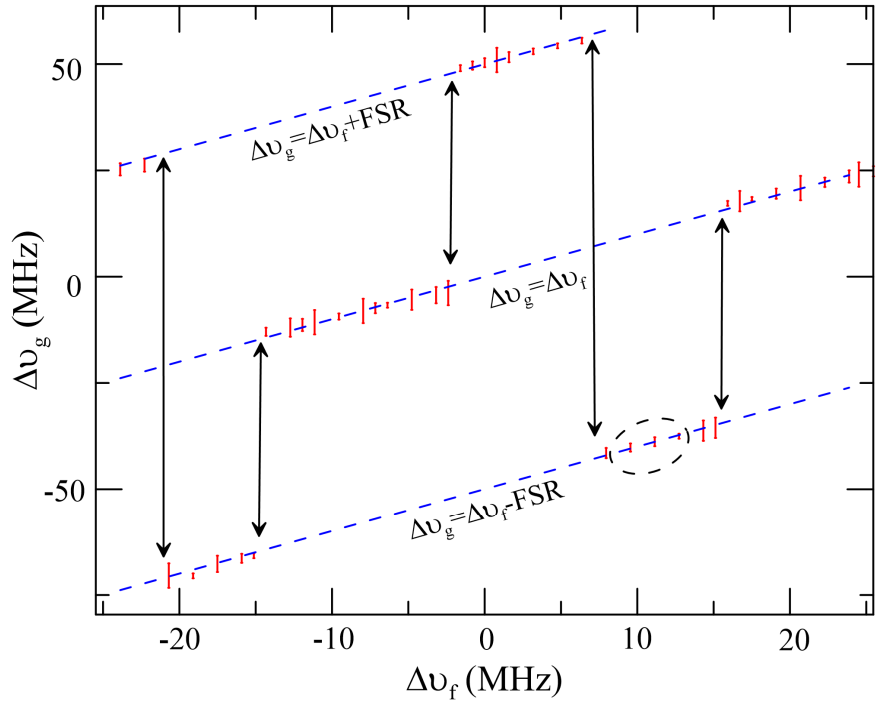

Figure 6. Change of the laser frequency with the detuning $\Delta\upsilon_f$: FWHM laser linewidth in a scale of 30:1 (bars); frequencies of three ring resonator transmission peaks (blue), jumps of the generation line (arrows); the selected range corresponds to Fig.5

Let us consider now the laser spectral performance at different feedback levels. Fig. 4 (a) demonstrates how the laser generation line changes as the feedback value increases from $l_{ext} = 6.25 \cdot 10^{-6}$ to $l_{ext} = 4 \cdot 10^{-4}$. One can see that at low feedback ($l_{ext} = 6.25 \cdot 10^{-6}$) the spectrum of the solitary laser is distorted, but the feedback induced threshold decrease is not enough to suppress laser generation at the solitary laser central frequency. Distortions of the laser spectrum occur at the frequencies corresponding to the modes of the ring resonator. In the region of the ring cavity mode closest to the center solitary laser frequency a destructive interference occurs leading to an increase of the generation threshold and formation of the spectral intensity dip. In the region of the second neighboring mode, a constructive interference occurs and the generation threshold is reduced, however, the value of the feedback is not enough to shift the generation frequency to this region. On the contrary, the laser generation peak shifts to the region of the nearest resonator mode, but the generation does not exhibit resonant character. With increasing feedback, $l_{ext} > 2 \cdot 10^{-5}$ the generation line shifts to the region of constructive interference and coincides with the resonator transmission peak (Fig. 4 (a)). Note that with increasing the feedback strength the generation stabilizes, i.e. both laser line narrowing and reduction of the background noise level occur. Besides, with the feedback increasing from $l_{ext} = 1 \cdot 10^{-4}$ to $l_{ext} = 4 \cdot 10^{-4}$ the laser narrowing is accompanied by laser frequency stabilization near the transmission peak of the resonator (Fig 4 (b)). This effect can be referred to as a frequency locking of the generation line. With further increase of the feedback $l_{ext} > 5 \cdot 10^{-4}$ a number of additional ring resonator modes are excited and the laser line is broadened, i.e. effects typical for "collapse of coherence" take place. Such laser operation is beyond the scope of this paper, so our further consideration is limited to feedback level of $l_{ext} = 4 \cdot 10^{-4}$.

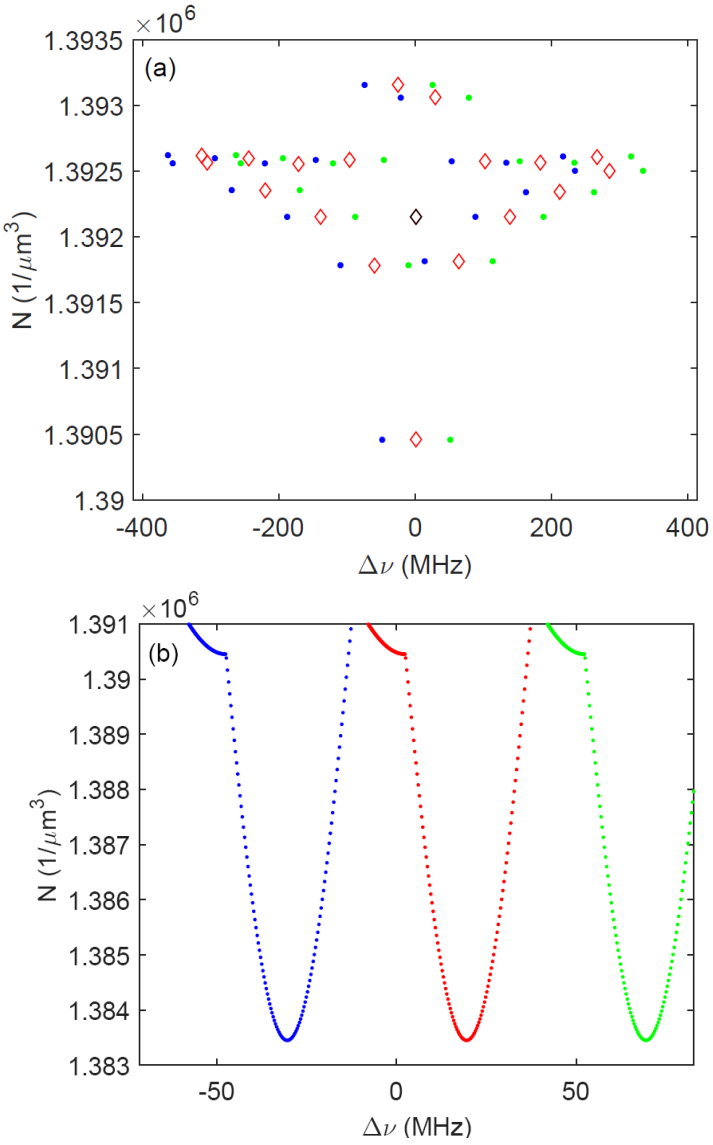

Fig. 7. (a) Compound modes in the plane frequency shift – carrier density for the system semiconductor laser – delayed fiber ring-cavity for zero frequency detuning. The black diamond is the solitary laser mode; the red diamonds denote the compound modes when a single fiber cavity mode with zero detuning to the laser mode is taken into account and the green (blue) dots denote the compound modes for the neighboring fiber cavity modes at a ± the fiber-cavity free spectral range (50 MHz) detuning; (b) Dependence of the three lowest carrier density modes in (a) on the frequency detuning $\Delta\upsilon_f$.

Let us analyze the specific features of the laser frequency locking with a change of the difference $\Delta\upsilon_f$ between the center solitary laser frequency and the nearest peak of the resonator transmission spectrum. Physically, such tuning can be associated with the temperature variations in the laser configuration or modulations of the laser currents (both laser diode current and thermocontroller current) leading to modifications of the ring resonator and laser diode cavity lengths.

Fig. 5 demonstrates laser generation lines obtained at different detuning frequencies $\Delta\upsilon_f$. One can see that due to the resonant properties of $f_{ext}(\omega)$ small changes of the generation frequency $\Delta\upsilon_f$ correspond to small changes of $\Delta\upsilon_f$, i.e. within a certain limit the laser generation line follows the peak of the ring resonator transmission. It is worth noting that the shift of the frequency corresponding to the constructive interference differs from the shift $\Delta\upsilon_f$, i.e. the laser generation line changes its position within the transmission peak in accordance with the nonlinear dependence of the frequency change $\Delta\upsilon_g$ on the feedback value (3).

The result shown in Fig. 6 is the main result of our analysis. It shows how changes of the laser generation frequency depend on the detuning $\Delta\upsilon_f$. Importantly, these dependencies are presented by a piecewise continuous curve that contain continuous "segments" typically in ten MHz range, and so the detuning of $\Delta\upsilon_f$ within one such "segment" smoothly changes the laser generation frequency that follows the position of the ring resonator transmittance peak.

Physically, this means that with temperature fluctuations or slow modulation of the operating currents within certain ranges, the described mechanism is able to stabilize lasing at the frequency strongly locked to the ring resonator transmission spectral peak maintaining as well the shape of the laser generation line. The laser generation linewidth is determined by the shape of the "potential well" associated with the resonator transmission peak directing the laser operation [37, 38]. The spontaneous emission noise could as well affect the constructive interference of the generated and reflected fields inside the semiconductor laser cavity causing laser line broadening. At some detuning values $\Delta\upsilon_f$ the conditions for laser generation at two neighboring resonator peaks becomes equal and in these points spontaneous noise provokes mode-hopping between two ring-resonator modes leading to a sudden change of the laser generation frequency by a value equal to the resonator free spectral range $\mathrm{FSR}=n_f L_r/c$. Obviously, stochastic mode hopping disturbs the laser stability and impairs its performance characteristics. In order to achieve a stable laser operation the system temperature and laser operation currents should be stabilized at the levels ensuring detuning $\Delta\upsilon_f$ within continuous "segments" of the curve shown in Fig. 6. These results allow to explain key features of the experimental observations [29] reported for a DFB laser with a narrowband feedback through a fiber ring interferometer. In particular, mode-hopping events periodically occurring in the experiments with a typical time interval of several seconds are associated with the thermally induced changes of mutual positions of the DFB laser cavity and external ring interferometer modes.

In order to get more inside in the compound modes of the whole semiconductor laser – resonant fiber-cavity system we find the steady state solution of the system in a manner similar to [34] but accounting for three fiber-cavity modes according to (4). For the laser and fiber cavity parameters listed in Tables 1 and 2 we obtained external cavity modes and antimodes as depicted in Fig. 7 (a) for three fiber-cavity modes. As can be seen, the lowest carrier density modes are the ones that are closest to the three fiber-cavity modes with frequency detuning of about 50 MHz. This, together with the result presented in Fig. 7(b), namely the dependence of the three lowest carrier density modes in (a) on the frequency detuning $\Delta\upsilon_f$ helps to explain the numerical result on mode hopping in Fig. 6 obtained by integration of (1). As the system generates light at the frequency of mode with the lowest carrier density, changing the frequency detuning leads to continuous shift the frequency of the lasing mode followed by an abrupt switching to the frequency of the neighboring modes (the blue and the green curves), i.e. to the mode hopping results in Fig. 6 obtained by numerical integration.

4. CONCLUSION

We report on a delayed rate equation model of a single-frequency semiconductor laser coupled to a fiber ring resonator [39, 40]. It is shown that, at a certain feedback level, the generation frequency of the semiconductor laser is locked to the spectral peak of the ring resonator transmission providing both strong laser line narrowing and a decrease of the noise level. It is also established that when the system parameters change leading to a mutual shift of the resonator transmission peaks and the solitary laser generation frequency (fiber length variation, current modulation) the laser frequency follows the resonator transmission peak changes. However, for a shift larger then a critical value the laser

frequency could jump between two stable positions associated with two resonator transmission peaks highlighting the laser mode-hoping. The described effects are in qualitative agreement with the experimental data [29] and are important for understanding of the physical mechanisms responsible for laser instabilities. Further development of such kind of lasers is extremely promising for applications in fiber-based sensor technologies, including local [41,42], distant [43] and distributed fiber sensing [44-49], where low-cost narrow-band laser sources with high stability are of particular demand.

ACKNOWLEDGMENT

The work was supported by Ministry of Education and Science of Russian Federation (14.Z50.31.0015, "State Assignment" 3.3889.2017), Russian Fund of Basic Research (16-42-732135 R-OFIM). K. P. is grateful to the Methusalem Foundation for financial support. A.F. acknowledges a support from the Leverhulme Trust (Visiting Professor, Grant ref: VP2-2016-042).

REFERENCES

[1] Luvsandamdin, E., Kürbis, C., Schiemangk, M., Sahm, A., Wicht, A., Peters, A., Erbert, G., Tränkle, G., "Micro-integrated extended cavity diode lasers for precision potassium spectroscopy in space," Optics Express 22(7), 7790 (2014).

[2] Numata, K., Camp, J., Krainak, M. A., Stolpner, L., "Performance of planar-waveguide external cavity laser for precision measurements," Optics Express 18(22), 22781 (2010).

[3] Baney, D. M., Szafraniec, B., Motamedi, A., "Coherent optical spectrum analyzer," IEEE Photonics Technology Letters 14(3), 355–357 (2002).

[4] Lu, B, Wei, F. . Zhang, Z. , Xu, D. , Pan, Z. , Chen, D. and Cai, H. ,"Research on tunable local laser used in ground-to-satellite coherent laser communication," Chin. Opt. Lett 13, 091402 (2015).

[5] Morin, M., Ayotte, S., Latrasse, C., Aubé, M., Poulin, M., Painchaud, Y., Gagnon, N. and Lafrance, G., "What narrow-linewidth semiconductor lasers can do for defense and security?," Fiber Optic Sensors and Applications VII, A. Mendez, H. H. Du, A. Wang, E. Udd, and S. J. Mihailov, Eds., SPIE (2010).

[6] Dahmani, B., Hollberg, L. and Drullinger, R., "Frequency stabilization of semiconductor lasers by resonant optical feedback," Optics Letters 12(11), 876 (1987).

[7] Spirin, V. V., Kellerman, J., Swart, P. L., Fotiadi, A. A., "Intensity noise in SBS with injection locking generation of Stokes seed signal," Optics Express 14(18), 8328 (2006).

[8] Liang, W., Ilchenko, V. S., Savchenkov, A. A., Matsko, A. B., Seidel, D., Maleki, L., "Whispering-gallery-mode-resonator-based ultranarrow linewidth external-cavity semiconductor laser," Optics Letters 35(16), 2822 (2010).

[9] Liang, W., Ilchenko, V. S., Eliyahu, D., Savchenkov, A. A., Matsko, A. B., Seidel, D., Maleki, L., "Ultralow noise miniature external cavity semiconductor laser," Nature Communications 6(1), 7371 (2015).

[10] Spirin, V. V., Castro, M., López-Mercado, C. A., Mégret, P., Fotiadi, A. A., "Optical locking of two semiconductor lasers through high-order Brillouin Stokes components in optical fiber," Laser Physics 22(4), 760–764 (2012).

[11] Spirin, V. V., López-Mercado, C. A., Bueno Escobedo, J. L., Márquez Lucero, A., Zolotovskii, I. O., Mégret, P., Fotiadi, A. A., "Self-injection locking of the DFB laser through ring fiber optic resonator," Fiber Lasers XII: Technology, Systems, and Applications, L. B. Shaw, Ed., SPIE 9344, 93442B (2015).

[12] Spirin, V. V., López-Mercado, C. A., Mégret, P., Fotiadi, A. A., "Single-mode Brillouin fiber laser passively stabilized at resonance frequency with self-injection locked pump laser," Laser Physics Letters 9(5), 377–380 (2012).

[13] Spirin, V. V., López-Mercado, C. A., Kinet, D., Mégret, P., Zolotovskiy, I. O., Fotiadi, A. A., "A single-longitudinal-mode Brillouin fiber laser passively stabilized at the pump resonance frequency with a dynamic population inversion grating," Laser Physics Letters 10(1), 15102 (2013).

[14] Spirin, V.V., Mégret, P., Fotiadi, A.A., "Passively Stabilized Doubly Resonant Brillouin Fiber Lasers," Fiber Lasers (M. Paul, J. Kolkata, eds), INTECH (2016).

[15] Spirin, V. V., López-Mercado, C. A., Kablukov, S. I., Zlobina, E. A., Zolotovskiy, I. O., Mégret, P., Fotiadi, A. A., "Single cut technique for adjustment of doubly resonant Brillouin laser cavities," Optics Letters 38(14), 2528 (2013).

[16] López-Mercado, C. A., Spirin, V. V., Kablukov, S. I., Zlobina, E. A., Zolotovskiy, I. O., Mégret, P., Fotiadi, A. A., "Accuracy of single-cut adjustment technique for double resonant Brillouin fiber lasers," Optical Fiber Technology 20(3), 194–198 (2014).
[17] López-Mercado, C. A., Spirin, V. V., Kablukov, S. I., Zlobina, E. A., Zolotovsky, I. O., Mégret, P., Fotiadi, A. A., "Adjustment of double resonance in short cavity Brillouin fiber lasers," Fiber Lasers XI: Technology, Systems, and Applications, S. Ramachandran, Ed., SPIE 6961, 89612V (2014).
[18] Preda, C. E., Fotiadi, A. A., Mégret, P., "Numerical approximation for Brillouin fiber ring resonator," Optics Express 20(5), 5783 (2012).
[19] Popov, S. M., Chamorovski, Y. K., Isaev, V. A., Mégret, P., Zolotovskii, I. O., Fotiadi, A. A., "Electrically tunable Brillouin fiber laser based on a metal-coated single-mode optical fiber," Results in Physics 7, 852–853 (2017).
[20] Fotiadi, A. A., Lobach, I. and Mégret, P., "Dynamics of ultra-long Brillouin fiber laser," Fiber Lasers X: Technology, Systems, and Applications, S. T. Hendow, Ed., SPIE 8601, 86011K (26 February 2013) (2013).
[21] Chernikov, S.V., Fotiadi, A.A., "Q-switching of fiber lasers with use of a dynamic SBS silica fiber mirror", Conference on Laser and Electro-Optics, 1997 Technical Digest Series, (Optical Society of America, Washington, D.C., 1997), 477-488 (1997).
[22] Lobach, I. A., Kablukov, S. I., Podivilov, E. V., Fotiadi, A. A., Babin, S. A., "Fourier synthesis with single-mode pulses from a multimode laser," Optics Letters 40(15), 3671 (2015).
[23] Fotiadi, A., Lobach, I., Megret, P.,"Acoustic and thermal effects in Brillouin Random Fiber Laser," in 2015 European Conference on Lasers and Electro-Optics - European Quantum Electronics Conference, (Optical Society of America, 2015), paper CJ-P.28 (2015)
[24] Popov, S. M., Chamorovsky, Y. K., Megret, P., Zolotovskii, I. O., Fotiadi, A. A., "Brillouin random lasing in artifice Rayleigh fiber," 2015 European Conference on Optical Communication (ECOC), IEEE (2015).
[25] Popov, S. M., Butov, O. V., Chamorovsky, Y. K., Megret, P., Zolotovskii, I. O., Fotiadi, A. A., "Short cavity Brillouin random laser," 2016 International Conference Laser Optics (LO), IEEE (2016).
[26] Lobach, I. A., Drobyshev, R. V., Fotiadi, A. A., Podivilov, E. V., Kablukov, S. I., Babin, S. A., "Open-cavity fiber laser with distributed feedback based on externally or self-induced dynamic gratings," Optics Letters 42(20), 4207 (2017).
[27] Popov, S. M., Butov, O. V., Chamorovskiy, Y. K., Isaev, V. A., Kolosovskiy, A. O., Voloshin, V. V., Vorob'ev, I. L., Vyatkin, M. Y., Mégret, P., Odnoblyudov, M., Korobko, D. A., Zolotovskii, I. O., Fotiadi, A. A., "Brillouin lasing in single-mode tapered optical fiber with inscribed Fiber Bragg Grating Array," Results in Physics, in press (2018).
[28] Popov, S. M., Butov, O. V., Chamorovskiy, Y. K., Isaev, V. A., Mégret, P., Korobko, D. A., Zolotovskii, I. O., Fotiadi, A. A., "Narrow linewidth short cavity Brillouin random laser based on Bragg Grating array fiber and dynamical population inversion gratings," Results in Physics, in press (2018).
[29] López-Mercado, C. A., Spirin, V. V., Bueno Escobedo, J. L., Márquez Lucero, A., Mégret, P., Zolotovskii, I. O., Fotiadi, A. A., "Locking of the DFB laser through fiber optic resonator on different coupling regimes," Optics Communications 359, 195–199 (2016).
[30] Bueno Escobedo, J. L., Spirin, V. V., López-Mercado, C. A., Mégret, P., Zolotovskii, I. O., Fotiadi, A. A., "Self-injection locking of the DFB laser through an external ring fiber cavity: Polarization behavior," Results in Physics 6, 59–60 (2016).
[31] Ohtsubo, J., [Semiconductor lasers: stability, instability and chaos], Springer Series in Optical Sciences, Springer Berlin Heidelberg (2013).
[32] K. Petermann, [Laser diode modulation and noise], Springer Science & Business Media (2012).
[33] Yousefi, M., Lenstra, D., Vemuri, G., "Nonlinear dynamics of a semiconductor laser with filtered optical feedback and the influence of noise," Physical Review E 67(4), 046213 (2003).
[34] Erzgräber, H., Krauskopf, B., Lenstra, D., Fischer, A. P., Vemuri, G., "Frequency versus relaxation oscillations in a semiconductor laser with coherent filtered optical feedback," Physical Review E 73(5), 055201 (2006).
[35] Schunk, N., Petermann, K., "Numerical analysis of the feedback regimes for a single-mode semiconductor laser with external feedback," IEEE Journal of Quantum Electronics 24(7), 1242–1247 (1988).

[36] Schunk, N., Petermann, K., "Noise analysis of injection-locked semiconductor injection lasers," IEEE Journal of Quantum Electronics 22(5), 642–650 (1986)
[37] Mork, J., Tromborg, B., "The mechanism of mode selection for an external cavity laser," IEEE Photonics Technology Letters 2(1), 21–23 (1990).
[38] Lenstra, D., "Statistical theory of the multistable external-feedback laser," Optics Communications 81(3–4), 209–214 (1991).
[39] Korobko, D. A., Zolotovskii, I. O., Panajotov, K., Spirin, V. V.,Fotiadi, A. A., "Self-injection-locking linewidth narrowing in a semiconductor laser coupled to an external fiber-optic ring resonator," Optics Communications 405, 253–258 (2017).
[40] Zolotovskii, I. O., Korobko, D. A., Fotiadi, A. A., Panajotov, K., "Frequency locking of a semiconductor laser by a ring fibre resonator," Quantum Electronics 47(10), 871–876 (2017).
[41] Fotiadi, A. A., Brambilla, G., Ernst, T., Slattery, S. A., Nikogosyan, D. N., "TPA-induced long-period gratings in a photonic crystal fiber: inscription and temperature sensing properties," Journal of the Optical Society of America B 24(7), 1475 (2007).
[42] Caucheteur, C., Fotiadi, A., Megret, P., Slattery, S. A., Nikogosyan, D. N., "Polarization properties of long-period gratings prepared by high-intensity femtosecond 352-nm pulses," IEEE Photonics Technology Letters 17(11), 2346–2348 (2005).
[43] Faustov, A. V., Gusarov, A. I., Mégret, P., Wuilpart, M., Kinet, D., Zhukov, A. V., Novikov, S. G., Svetukhin, V. V., Fotiadi, A. A., "Gamma radiation-induced blue shift of resonance peaks of Bragg gratings in pure silica fibres," Quantum Electronics 46(2), 150–154 (2016).
[44] Faustov, A. V., Gusarov, A. V., Mégret, P., Wuilpart, M., Zhukov, A. V., Novikov, S. G., Svetukhin, V. V., Fotiadi, A. A., "The use of optical frequency-domain reflectometry in remote distributed measurements of the γ-radiation dose," Technical Physics Letters 41(5), 414–417 (2015).
[45] Faustov, A. V., Gusarov, A. V., Mégret, P., Wuilpart, M., Zhukov, A. V., Novikov, S. G., Svetukhin, V. V., Fotiadi, A. A., "Application of phosphate doped fibers for OFDR dosimetry," Results in Physics 6, 86–87 (2016).
[46] Bueno Escobedo, J. L., Spirin, V. V., López-Mercado, C. A., Márquez Lucero, A., Mégret, P., Zolotovskii, I. O., Fotiadi, A. A., "Self-injection locking of the DFB laser through an external ring fiber cavity: Application for phase sensitive OTDR acoustic sensor," Results in Physics 7, 641–643 (2017).
[47] Bueno Escobedo, J. L., Spirin, V. V., López-Mercado, C. A., Marquez Lucero, A., Mégret, P., Zolotovskii, I. O., Fotiadi, A. A., " New fiber laser design for application in phase sensitive optical time domain reflectometry ," Optical Sensors 2017, F. Baldini, J. Homola, and R. A. Lieberman, Eds., SPIE 10231, 1023129 (2017).
[48] V.V. Spirin, C. López-Mercado, P. Mégret, A.A. Fotiadi, "Fiber laser for phase sensitive optical time domain reflectometry," [Optical Fiber, Ed. Fei Xu], 2018.
[49] Spirin, V. V., Bueno Escobedo, J. L., Korobko, D., Zolotovskiy, I., López-Mercado, C., Mégret, P., Fotiadi, A. A., "Fiber laser for application in phase sensitive optical time domain reflectometry," Fiber Lasers XV: Technology and Systems, A. L. Carter and I. Hartl, Eds., SPIE 10512, 105122F (2018).